Protein J (2010) 29:365–372
DOI 10.1007/s10930-010-9261-5

Site-Saturation Mutagenesis of Leucine 134 of *Bacillus licheniformis* Nucleotide Exchange Factor GrpE Reveals the Importance of this Residue to the Co-chaperone Activity

Min-Guan Lin · Bo-En Chen · Wan-Chi Liang · Wei-Mou Chou · Jiau-Hua Chen · Lih-Ying Kuo · Long-Liu Lin

Published online: 16 June 2010

Abstract To elucidate the role of leucine 134 of *Bacillus licheniformis* nucleotide exchange factor (*Bl*GrpE), site-saturation mutagenesis was employed to generate all possible replacements for this residue. Wild-type and mutant proteins were purified by nickel-chelated chromatography and had a molecular mass of approximately 34.5 kDa. As compared with wild-type *Bl*GrpE, the nucleotide exchange factor (NEF) activity of L134H, L134K, L134R, L134D, L134E, L134N, L134Q, L134S, L134G and L134P was reduced by more than 96%. In vitro binding assay revealed that wild-type *Bl*GrpE and the functional variants mainly interacted with the monomer of *Bl*DnaK, but no such interaction was observed for the remaining mutant proteins. *Bl*GrpE and 9 mutant proteins synergistically stimulated the ATPase activity of *B. licheniformis* DnaK (*Bl*DnaK), whereas the NEF-defective variants had no synergistic stimulation. Comparative analysis of the far-UV CD spectra showed that the α-helical content of the inactive mutant *Bl*GrpEs was reduced significantly with respect to wild-type protein. Moreover, the inactive mutant proteins also exhibited a more sensitivity towards the temperature-induced denaturation. Taken together, these results indicate that Leu134 might play a structural role for the proper function of *Bl*GrpE.

Keywords *Bacillus licheniformis* · GrpE · Site-saturation mutagenesis · Co-chaperone activity · Temperature-induced denaturation

Abbreviations

Hsp70	Heat shock protein 70
NEF	Nucleotide exchange factor
*Ec*DnaK	*Escherichia coli* DnaK
*Ec*GrpE	*E. coli* GrpE
NBD	Nucleotide-binding domain
*Bl*GrpE	*Bacillus licheniformis* GrpE
*Bl*DnaK	*B. licheniformis* DnaK
Ni^{2+}-NTA	Ni^{2+}-nitrilotriacetate
IPTG	Isopropyl-β-D-thiogalactopyranoside
PAGE	Polyacrylamide gel electrophoresis
*Bl*DnaJ	*B. licheniformis* DnaJ

1 Introduction

Molecular chaperones are involved in various cellular functions including protein folding, refolding/degradation of nonnative proteins, prevention of protein aggregation under stress condition, and regulation of protein activities [18]. Heat shock protein 70 (Hsp70) is a ubiquitous

Min-Guan Lin and Bo-En Chen contributed equally to this work.

M.-G. Lin · W.-M. Chou
Department of Biochemical Science and Technology, National Chiayi University, 300 University Road, Chiayi 60004, Taiwan

B.-E. Chen · W.-C. Liang · L.-L. Lin (✉)
Department of Applied Chemistry, National Chiayi University, 300 University Road, Chiayi 60004, Taiwan
e-mail: llin@mail.ncyu.edu.tw

J.-H. Chen
Department of Food Science and Technology, Chia-Nan University of Pharmacy and Science, Tainan, Taiwan

L.-Y. Kuo
Department of Food Science and Applied Biotechnology, Hungkuang University, Shalu, Taichung, Taiwan

molecular chaperone family widely distributed in the three domains of life. Hsp70 is an ATP-dependent molecular chaperone that exhibits weak intrinsic ATPase activity and the protein is usually present in an ATP-bound state [27]. Although Hsp70 has low affinity together with fast exchange rates for substrates in the ATP-bound state, ADP-bound Hsp70 undergoes an internally conformational change that results in comparatively high affinity coupled with slow exchange rates towards substrates [8]. This structural alteration of Hsp70 is tied with ATP hydrolysis and ADP/ATP exchange, which is closely related to the actions of the co-chaperones J-protein and nucleotide exchange factor (NEF) [8]. Both cooperative proteins are essential for the efficient progression of the molecular chaperone cycle.

In prokaryotes, *Escherichia coli* DnaK (*Ec*DnaK) is a well-known Hsp70 counterpart whose ATPase activity is mediated by an Hsp40 protein, DnaJ, in synergy with substrate binding [9]. It has been shown that ADP dissociation from *Ec*DnaK is accelerated 5,000-fold by an NEF homologue, GrpE [36] and such action leads to the efficient ATP rebinding to the molecular chaperone and substrate release [26]. *E. coli* GrpE (*Ec*GrpE) consists of a homodimeric structure with a very unusual and unique feature of two long α-helices at the N-terminal end paired together in a non-coiled parallel arrangement [17]. This tail region of the structure has been shown to act as a thermosensor in the temperature-regulated action of the DnaK/DnaJ/GrpE heat shock system [14, 40]. There is also a four-helix bundle formed at the dimer interface with each monomer contributing two α-helices and it has been shown that the bundle serves as a scaffold for the association of the long helices [12, 30]. The crystal structure has demonstrated a direct interaction between *Ec*GrpE and the nucleotide-binding domain (NBD) of *Ec*DnaK, suggesting a forced opening of the nucleotide-binding cleft of *Ec*DnaK by insertion of the *β*-sheet domain of *Ec*GrpE [17]. Very recently, the structure of *Thermus thermophilus* GrpE was determined at 3.23-Å resolution and has shed still more light on the topology of this protein group [35].

Earlier, a recombinant *B. licheniformis* GrpE (*Bl*GrpE) was expressed in *E. coli* cells [23], and a double mutant *Bl*GrpE (*Bl*GrpE-L52P/L134H) with no co-chaperone function was also characterized [22]. In order to do a further investigation at leucine 134 of *Bl*GrpE, we performed saturation mutagenesis on this position. Surprisingly, it was found that some replacements were detrimental to the structural integrity of *Bl*GrpE. This clearly brings into the suggestion that Leu134 is necessary for *Bl*GrpE to function as a co-chaperone. The saturation mutagenesis also indentified the functionally competent replacements that had a comparable co-chaperone activity with respect to wild-type *Bl*GrpE.

2 Materials and Methods

2.1 Materials, Bacterial Strains, and Growth Conditions

Luria-Bertani (LB) media for bacterial culture were acquired from Difco Laboratories (Detroit, MI, USA). A QuikChange II site-directed mutagenesis kit for mutagenic PCR amplification was purchased from Stratagene (La Jolla, CA, USA). Protein assay reagents were obtained from Bio-Rad Laboratories (Hercules, CA, USA). Ni^{2+}-nitrilotriacetate (Ni^{2+}-NTA) resin was acquired from Qiagen Inc. (Valencia, CA, USA). Unless otherwise noted, all other chemicals were commercial products of analytical grade or molecular biological grade.

Escherichia coli NovaBlue (Novagen Inc., Madison, WI, USA) was used in the preparation of plasmids and *E. coli* XL-1 Blue (Stratagene) was used for site-directed mutagenesis. T5 RNA-polymerase-mediated gene expression was performed in *E. coli* M15 (pRep4) (Qiagen). *E. coli* strains were grown aerobically in LB medium at either 20 or 37 °C. As required, ampicillin and kanamycin were supplemented to a final concentration of 100 and 25 μg/ml, respectively.

2.2 Saturation Mutagenesis

The L134X-mutated *grpE* genes from *B. licheniformis* were constructed on the expression plasmid pQE-*Bl*GrpE [23] by oligonucleotide-directed mutagenesis using the following complementary primers: 5′-ATTTTGGAGGCT NNNAAAAATGAAGGAGTT-3′ and 5′-AACTCCTTCA TTTTTNNNAGCCTCCAAAAT-3′. Underlined sequences, which encode codon at site 134, were randomized for saturation mutagenesis. Mutant DNAs were generated with a thermocycling program of 2 min at 95 °C and 16 cycles of 30 s at 95 °C, 60 s at 55 °C, and 12 min at 68 °C on an Applied Biosystems thermal cycler. The amplified products were digested with 10 units of *Dpn*I at 37 °C for 1 h, prior to their use for transformation into *E. coli* XL-1 blue cells. Mutations were confirmed by DNA sequencing, which was carried out with dye terminator sequencing kit and an automatic DNA sequencer (Applied Biosystems, Foster City, CA, USA).

2.3 Expression and Purification of Wild-type and Mutant Proteins

To express wild-type and mutant *Bl*GrpEs, plasmid constructions were transformed into the *E. coli* M15 (pRep4). Transformed cells were grown at 37 °C, with shaking in LB broth containing 100 μg ampicillin/ml and 25 μg kanamycin/ml, until a cell density (optical density at

600 nm) of 0.6–0.8 was reached. Flasks containing the cultures were supplemented with isopropyl-β-D-thiogalactopyranoside (IPTG) at a final concentration of 1 mM. Cells were then cultured at 20 °C for 14 h with vigorous shaking. Cells were collected and pellets were resuspended in a buffer containing 50 mM Tris–HCl, 300 mM NaCl, and 10 mM imidazole buffer at pH 7.0. Cells were lysed by sonication (30-s bursts and pulses for 5 min), and cell debris was removed by centrifugation at 12,000*g*. Recombinant proteins were purified by affinity chromatography using a Ni^{2+}-NTA agarose column (Qiagen) under native conditions.

B. licheniformis DnaK (*Bl*DnaK) and DnaJ (*Bl*DnaJ) were expressed and purified as described previously [23]. To remove nucleotides bound to *Bl*DnaK, the purified protein (0.24 mg/ml) was diluted with 50 mM Tris-HCl buffer (pH 7.0) to 50 ml, and ten units of alkaline phosphatase (Promega Corp., Madison, WI, USA) were added and allowed to react at room temperature for one hour. Then, the solution was concentrated to 5 ml using an Amicon stirred cell equipped with YM-10 membrane (Millipore Corp., Billerica, MA, USA) and applied to a Superdex 200-gel filtration column (Pharmacia) for removal of alkaline phosphatase. After analysis of the steady-state turnover rate of ATP by a coupled colorometric assay [1], protein fractions with a turnover number of at most 1.5×10^{-3} s^{-1} were pooled and stored at −70 °C until use.

2.4 Electrophoresis and Determination of Protein Concentration

Polyacrylamide gel electrophoresis (PAGE) was performed on 7.5% native-gel and 12% SDS-gel using a mini-slab gel system (Mini Protean III; Bio-Rad). Following electrophoresis, the proteins were stained with Coomassie Brilliant Blue-250 and destained with a methanol (30%) and acetic acid (10%) solution. The protein standards used for estimation of molecular masses were rabbit phosphorylase *b* (97.4 kDa), bovine serum albumin (66.2 kDa), chicken egg albumin (45.0 kDa), bovine carbonic anhydrase (29.0 kDa), and trypsin inhibitor (20.1 kDa).

Protein concentrations were determined using the Bio-Rad protein assay based on the Bradford dye-binding procedure [6] with bovine serum albumin as the standard.

2.5 Nucleotide Release Measurements

Nucleotide release experiments of the fluorescent nucleotide analog MABA-ADP (MoBiTec GmbH, Goettingen, Germany) was performed with an SX20 stopped-flow spectrometer (Applied Photophysics, Surrey, UK) as described elsewhere [7]. To obtain spontaneous nucleotide release rates, 2.5 μM *Bl*DnaK-MABA-ADP was mixed at 30 °C with an equal volume of 250 μM ADP (both in 50 mM Tris–HCl buffer, pH 7.0, containing 50 mM KCl and 5 mM $MgCl_2$). The nucleotide exchange activity of wild-type and mutant *Bl*GrpEs was assayed by adding the protein samples to the ADP solution and subsequently mixed with *Bl*DnaK-MABA-ADP complex. Release of labeled nucleotides was monitored by the decrease in fluorescence of the unbound MABA-ADP (excitation at 360 nm and cutoff filter at 420 nm).

2.6 ATPase Activity Assay

Steady-state ATPase activity assays were performed according to the malachite green method [21] with slight modifications. The reaction mixture contained 10 mM Hepes buffer (pH 7.0), 100 mM KCl, 2.5 mM $MgCl_2$, 1 mM ATP and 25 μM purified *Bl*DnaK. The release of free phosphate was recorded by monitoring the color changes at 660 nm. The assays were corrected for spontaneous ATP degradation. ATPase activity is defined as pmol ATP pmol *Bl*$DnaK^{-1}$ min^{-1} under the assay conditions.

Mutational effects on the ATPase activity of *Bl*DnaK (25 μM) were investigated in the presence of *B. licheniformis* DnaJ (*Bl*DnaJ) and NR-peptide (NRLLLTG). The reaction mixture contained the above-mentioned buffer system, 100 μM each of the recombinant *Bl*GrpEs, 25 μM *Bl*DnaK, 50 μM *Bl*DnaJ, and 50 μM NR-peptide. The ATPase activity was determined under the standard assay conditions.

2.7 Circular Dichroism (CD) Studies

Far-UV CD experiments were performed on a JASCO J-815 spectropolarimeter equipped with a temperature-controlling system. A stock of *Bl*GrpE or its derivatives was diluted in 10 mM Hepes buffer (pH 7.0) to a final concentration of 30 μM. Spectral analysis was taken over the wavelength range from 190 to 250 nm in cuvettes with a 2-mm path length at 0.2-nm intervals with 4-s integration time and a bandwidth of 2.0 nm. All of the measurements were performed under nitrogen flow. Each scanning was repeated four times and an average was obtained. Data were corrected for the effect of buffer, and the results were expressed as mean residue ellipticity $[\theta]$ in the unit of degrees cm^2 $dmol^{-1}$, which is defined as $[\theta] = M \times \theta/(100 \times c \times l)$, where M is the average molecular mass of amino acids, θ is the observed ellipticity in degrees, c is the concentration in residue moles per liter, and l is the length of the light path in centimeters. The secondary structural contents were estimated by the online DICHROWEB server (http://public-1.cryst.bbk.ac.uk/cdweb/htm1/, accessed on March 4, 2010) [25, 45] using the implemented CDSSTR program.

The unfolding transition curves for the recombinant proteins were obtained by measuring the ellipticity at 222 nm in a 1-mm cell at a protein concentration of 35 μM. The temperature was increased with a heating rate of 1 °C/min from 20 to 90 °C. For refolding experiments, the temperature was decreased by 1 °C/min and measurements were taken once every min. Thermal denaturation curves were fitted to a modified form of the van't Hoff equation, which simultaneously fits the native and denatured baselines and the transition region to obtain the T_m and ΔH values for denaturation [16]:

$$\Delta\varepsilon = (m_n T + b_n) + (m_d T + b_d)\left(\frac{K}{1+K}\right)$$

where

$$K = \exp[-\Delta H(1 - T/T_m)/RT]$$

Here, m_n and m_d, and b_n and b_d are the slopes and intercepts of the native- and denatured-state baselines respectively and T is the temperature.

3 Results and Discussion

3.1 Sequence Comparison

Intensive biochemical and structural studies of GrpE proteins provide a solid foundation for the investigation into the residues or regions crucial for the co-chaperone activity [33, 38, 42, 46–48]. The lack of structural data for *Bl*GrpE has invited speculations about possible similarities to other GrpE proteins. In this study, we aligned the amino acid sequence of *Bl*GrpE with that of *Ec*GrpE, whose three-dimensional structure has been determined [17]. By performing the program CLUSTLAW from ExPASy Proteomics server (http://tw.expasy.org), we observed that the *Bl*GrpE sequence shares 29% identity with the primary sequence of *Ec*GrpE. The alignment also indicated these two GrpE proteins have common structural features, especially the domain organization, with the N-terminal long α-helix, four-helix bundle, and C-terminal β-sheet domains arranged in order (Fig. 1). Therefore, it can be expected that the fundamental mechanism of the NEF reaction for DnaK by GrpE is sufficiently conserved between *B. licheniformis* and *E. coli* DnaK systems. As shown in Fig. 1, Leu134 is located at the boundary of the α3-helix of *Bl*GrpE. However, the role of this residue to the co-chaperone activity of *Bl*GrpE remains unclear. A further investigation will contribute a more comprehensive understanding to its importance in *Bl*GrpE function.

3.2 Site-saturation Mutagenesis and Purification of the Recombinant Proteins

Site-saturation mutagenesis provides a platform for the rapid diversification of protein traits [31]. This approach makes all possible mutations at one or pre-determined target positions and has been used successfully for in vitro directed evolution of various proteins [3, 20, 31, 37]. In this study, site-saturation mutagenesis at leucine 134 was employed to investigate in greater depth the contribution of this residue to the co-chaperone function of *Bl*GrpE. A library of *Bl*GrpE variants was created by overlap extension PCR using two degenerate synthetic oligonucleotides in which the target site (codon 134) was diversified with a randomized NNN codon. The library was subsequently screened by DNA sequencing for clones with the desired mutations. After the screening, pQE-*Bl*GrpE and each of the mutated plasmids were transformed into *E. coli* M15 (pRep4) for IPTG-induced gene expression. The expression of wild-type and mutant *Bl*GrpEs was assessed by analyzing protein profiles of the crude extracts. Both wild-type and mutant *Bl*GrpEs were expressed as a predominant band with an estimated molecular mass of 34.5 kDa (data not

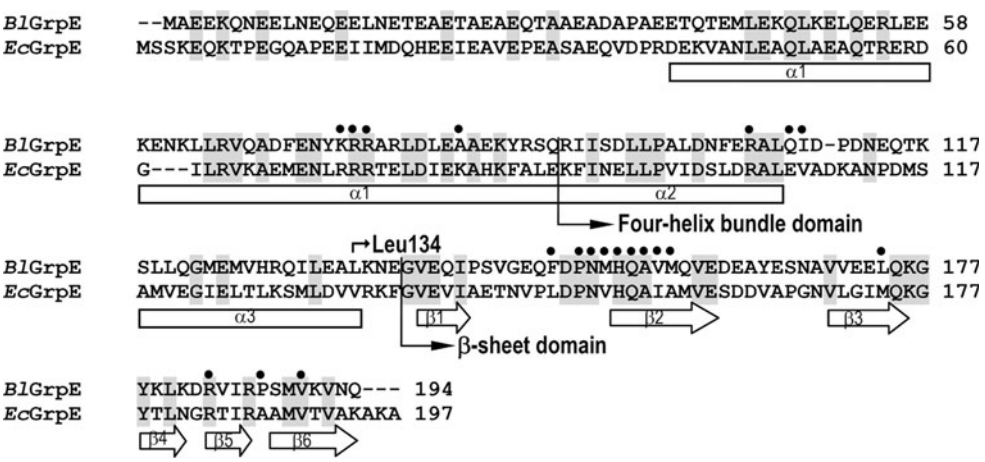

Fig. 1 Amino acid sequence alignment of *Bl*GrpE and *Ec*GrpE proteins. Based on the crystal structure of *Ec*GrpE, the secondary-structure elements of *Bl*GrpE are illustrated below the sequences. The identical residues are shaded and *Ec*GrpE residues interacting with *Ec*DnaK in the crystal structure of their complex are represented with *closed circles* [7]

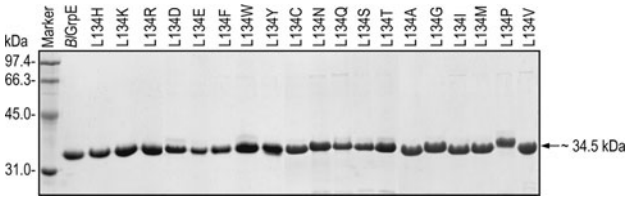

Fig. 2 Analysis of wild-type and mutant *Bl*GrpEs by SDS-PAGE. The protein samples (approximately 1.8 μg for each sample) were analyzed by 12% polyacrylamide-SDS gels and visualized by Coomassie brilliant staining

shown), which is inconsistent with the expected molecular mass of approximately 23.8 kDa. These results indicate that the recombinant *Bl*GrpEs displayed an abnormal mobility on SDS-PAGE. Interestingly, the anomalous electrophoretic behavior has also been observed in His_6-tagged GrpE from *E. coli* [41]. Few acidic proteins, such as ribonuclease U2 [11], α-synuclein [34], Gir2 [2] and rhizopuspepsin [10], have high content of acidic amino acids (14-25%) and migrate slower than expected. *Bl*GrpE also contains high proportion of acidic amino acids (23.4%), which may be responsible for its slower migration on SDS-PAGE. Wild-type and mutant proteins in the crude extracts were further purified to near homogeneity by Ni^{2+}-NTA resin (Fig. 2). The purification procedure resulted in a final yield of approximately 5–11 mg protein per liter of cell culture.

3.3 Functional Analysis of Wild-type and Mutant *Bl*GrpEs

To evaluate the mutational effects on the functionality of *Bl*GrpE, wild-type and mutant proteins were tested for nucleotide exchange activity on *Bl*DnaK using the stopped-flow assay. As shown in Table 1, the release rate of MABA-ADP was reduced more than 96% relative to wild-type *Bl*GrpE when Leu134 of the protein was replaced with His, Lys, Arg, Asp, Glu, Asn, Gln, Ser, Gly, and Pro. Additionally, the dramatic loss of NEF activity was correlated with the incapable binding of the mutant proteins to *Bl*DnaK (Table 1). These findings suggest that residue Leu134 of *Bl*GrpE is essential for the functional and physical interactions with *Bl*DnaK.

3.4 DnaK-binding Ability of Wild-type and Mutant *Bl*GrpEs

In solution, GrpE is an elongated homodimer that consists of an N-terminal unstructured region of unknown function, a long α-helix that forms two coils in the dimer, a four-helix bundle with two helices from each monomer responsible for protein dimerization and a C-terminal compact β-sheet domain [17]. The nucleotide exchange activity is based on its interaction with DnaK that induces a 14° outward rotation of subdomain IIB, disrupting the nucleotide-binding site and decreasing the affinity for ADP. In the three dimensional structure of the *Ec*DnaK$_{NBD}$:*Ec*GrpE complex, the dimer is asymmetric and the contacts are situated within the β-sheet and four-helix bundle subdomains of *Ec*GrpE [17]. Partial proteolysis and substrate dissociation kinetics further suggest that the N-terminal half of *Ec*GrpE interacts with the interdomain linker of *Ec*DnaK, regulates the nucleotide exchange activity of the co-chaperone and is required to stabilize DnaK-substrate complexes in the ADP-bound conformation [33].

To evaluate the interactions between *Bl*DnaK and the purified *Bl*GrpEs, each (~15 μM) of the recombinant proteins in 10 mM Hepes buffer (pH 7.0) containing 100 mM KCl, 2.5 mM $MgCl_2$, and 0.5 mM DTT was

Table 1 Effect of mutations on nucleotide exchange, DnaK-binding, and co-chaperone activities of *Bl*GrpE

Enzyme	Relative release rate (%)[a]	DnaK-binding activity[b]	Synergistic stimulation[c] (fold)
Wild-type	100 ± 5.6	+	12.93 ± 0.59
L134H	2.1 ± 0.3	−	1.70 ± 0.05
L134K	1.5 ± 0.1	−	1.25 ± 0.08
L134R	1.7 ± 0.2	−	1.52 ± 0.08
L134D	2.2 ± 0.4	−	1.74 ± 0.07
L134E	1.6 ± 0.2	−	1.42 ± 0.07
L134F	108.9 ± 9.1	+	14.77 ± 0.08
L134W	91.1 ± 3.9	+	10.68 ± 0.01
L134Y	96.7 ± 4.1	+	12.19 ± 0.16
L134C	112.8 ± 11.9	+	14.95 ± 0.74
L134N	2.8 ± 0.9	−	2.02 ± 0.12
L134Q	3.1 ± 0.7	−	3.11 ± 0.14
L134S	1.8 ± 0.6	−	1.59 ± 0.11
L134T	57.5 ± 7.3	+	7.43 ± 0.60
L134A	69.1 ± 8.2	+	8.93 ± 0.32
L134G	3.1 ± 0.7	−	3.97 ± 0.40
L134I	99.3 ± 10.2	+	13.09 ± 0.38
L134M	99.7 ± 9.8	+	13.05 ± 0.44
L134P	1.6 ± 0.1	−	2.13 ± 0.16
L134V	95.9 ± 5.7	+	12.41 ± 0.47

[a] The average nucleotide exchange activity of wild-type *Bl*GrpE was set to 100%

[b] The DnaK-binding ability was defined as the protein sample that could bind exclusively to the monomer of *Bl*DnaK. Symbols: +, binding; −, no binding

[c] The assay was performed at 40 °C with ATP at a final concentration of 1 mM. The reaction mixture contained 25 μM *Bl*DnaK, 50 μM *Bl*DnaJ, 100 μM each of the recombinant *Bl*GrpEs, and 50 μM NR-peptide. The intrinsic ATPase activity of *Bl*DnaK in the presence of wild-type *Bl*GrpE was used as a control

incubated with the molecular chaperone (7 μM) at 4 °C for 40 min. These samples were then subjected to gel electrophoresis under native conditions. Interestingly, the electrophoretic migrations for the monomeric form of wild-type and mutant *Bl*GrpEs showed a significant difference (data not shown), especially L134R, L134D, L134E and L134 N, although they had a similar molecular mass. It should be noted that the monomer was the predominant form of *Bl*Dnak, with a small fraction of other oligomeric species. Oligomerization is a common feature of Hsp70 homologs including Hsc70 [4], *Ec*DnaK [39], and *Agrobacterium tumefaciens* DnaK [5]. Non-denaturing PAGE analysis also revealed that wild-type *Bl*GrpE and the functional variants were specifically bound to the monomer of *Bl*DnaK (Table 1). However, non-specific bindings to *Bl*Dnak were observed in L134H, L134K, L134R, L134D, L134E, L134N, L134Q, L134S, L134G and L134P, implying that the relevant replacements result in the significant changes in the *Bl*GrpE structure.

3.5 Co-chaperone Activity of the Purified *Bl*GrpEs

It has been demonstrated that the chaperone function of DnaK is based on the substrate-binding and -release cycles, which are tightly regulated by nucleotides and co-chaperones DnaJ and GrpE [24, 28, 43]. In the ATPase cycle of DnaK, ATP-hydrolysis step and nucleotide-exchange step are rate-limiting processes in which DnaJ accelerates the hydrolysis rate of the DnaK-bound ATP and GrpE increases the release rate of bound ADP without affecting the rate of ATP hydrolysis. By their synergistic function, the apparent ATPase activity of DnaK is greatly stimulated in the presence of co-chaperones. In this regard, co-chaperone activity of GrpE should be evaluated to confirm whether the mutant proteins are active. The intrinsic specific ATPase activity for *Bl*DnaK was determined to be 0.39 ± 0.05 pmol ATP pmol *Bl*Dnak^{-1} min^{-1}. Upon the addition of wild-type *Bl*GrpE, the specific activity was increased to 0.97 ± 0.07 pmol ATP pmol *Bl*Dnak^{-1} min^{-1}. As compared with wild-type *Bl*GrpE only, the simultaneous addition of *Bl*DnaJ and *Bl*GrpE synergistically stimulated the ATPase activity of *Bl*DnaK by 8.7-fold (data not shown) and a further enhancement (12.5-fold) was observed by the incorporation of NR-peptide into the reaction mixture (Table 1). Similar to wild-type *Bl*GrpE, the ATPase activity of *Bl*DnaK was stimulated by more than 12-fold in the presence of some mutant *Bl*GrpEs (including L134F, L134Y, L134C, L134I, L134M and L134V), *Bl*DnaJ, and NR-peptide. However, the incorporation of L134H, L134K, L134R, L134D, L134E, L134N, L134Q, L134S, L134G, and L134P had no significant stimulation on the ATPase activity of *Bl*DnaK. These results suggest that some replacements, especially the introduction of a polar group or a charge group into position 134, had impaired the functionality of *Bl*GrpE.

3.6 Structural Analyses

To analyze how the secondary structure of *Bl*GrpE was affected by the mutations, we measured far-UV CD properties of wild-type and mutant proteins. The CD spectrum of *Bl*GrpE displays strong peaks of negative ellipticity at 208 and 222 nm indicative of substantial α-helical content (Fig. 3). This spectrometric characteristic strongly resembles those of GrpE counterparts from *E. coli* [12], *T. thermophilus* [15], *Chlamydomonas reinhardtii* chloroplast [46], and yeast mitochondria [32]. Most of the mutant *Bl*GrpEs had a CD spectrum comparable to the wild-type protein, whereas the ellipticity was reduced greatly in L134D, L134E, L134H, L134N, L134P, L134Q, and L134R (Fig. 3). The spectra were further quantitatively analyzed by the DICHROWEB server. The normalized root-mean-square deviation values of the data fitting for wild-type and mutant *Bl*GrpEs were all <0.1 units and thus showed excellent quality of the fit parameters [29]. The helical contents of *Bl*GrpE, L134Y, L134W, L134F, L134C, L134V, L134M, and L134I were 50, 47, 47, 57, 64, 46, 56, and 54%, respectively, and the β-sheet contents were 13, 11, 13, 8, 9, 10, 11, and 20%, respectively. The calculated helical and β-sheet contents of *Bl*GrpE were similar to the data derived from the crystal structure of GrpE counterpart from *E. coli* (PDB code: 1dkg). It is worth noting that the helical contents of inactive mutant *Bl*GrpEs were apparently lower than that of wild-type *Bl*GrpE (data not shown). These values confirm that the

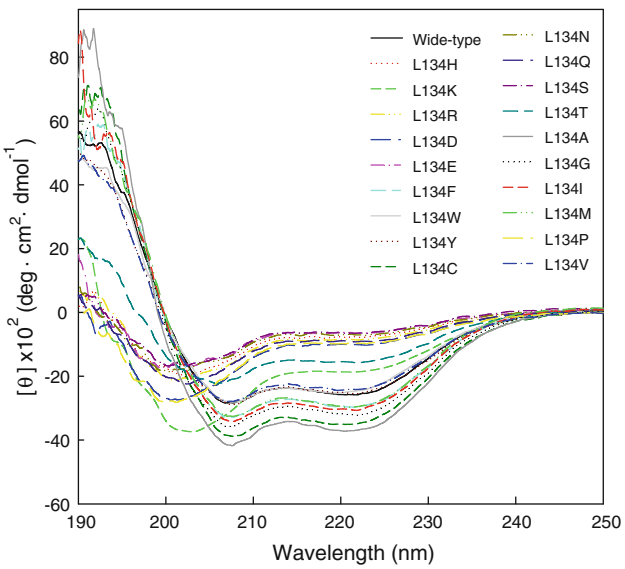

Fig. 3 CD spectra of wild-type and mutant *Bl*GrpEs. The far-UV CD spectra were recorded at 22 °C

significant changes in the secondary structure of *Bl*GrpE have been occurred as a consequence of L134R/K/H/E/D/T/S/Q/N/P mutations.

As noted by Grimshaw et al. [13], *Ec*GrpE is the only component of the DnaK system that undergoes conformational changes in the physiological temperature range. Conformational changes of *Ec*GrpE are fully reversible and it becomes transiently unable to interact with the NBD of *Ec*DnaK at heat-shock temperatures, leading to stabilization of the DnaK-ADP-substrate complex. In this regard, the temperature-induced unfolding transitions of wild-type and mutant *Bl*GrpEs followed by the loss of ellipticity at 222 nm with increasing temperature was investigated (Fig. 4). The transition for wild-type *Bl*GrpE started at ~42 °C and had its midpoint at 58 °C. It has been reported that *Ec*GrpE has two thermal transitions with the midpoint temperatures at 53 and 83 °C [10]. The first transition was proposed to attribute the unfolding of the paired α-helices and the second transition was assumed to involve in the unfolding of the four-helix bundle and dissociation of the dimer [12, 13]. However, only one fully reversible transition was observed in a GrpE homolog of yeast mitochondria and this transition was believed to be responsible for unfolding and dimer dissociation of the protein [32]. Consistent with the counterpart of yeast mitochondria, wild-type and mutant *Bl*GrpEs showed only one transition and this transition was highly reversible (data not shown). The functional mutant *Bl*GrpEs had their T_m values comparable to the wild-type protein, whereas the midpoint temperatures for the inactive variants were dramatically reduced to less than 47 °C. These results clearly indicate

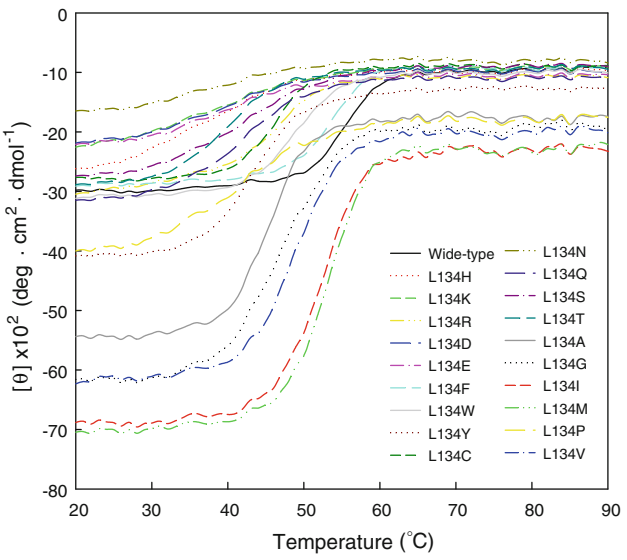

Fig. 4 Temperature denaturation of wild-type and mutant *Bl*GrpEs dissolved in 50 mM Tris–HCl buffer (pH 7.0) as monitored by the CD signal at 222 nm

that substitution of leucine 134 with polar or charged amino acids has a detrimental effect on the thermal stability of *Bl*GrpE.

The thermodynamic parameters of the inactivation process were also analyzed. As shown in Table 2, the ΔH value for wild-type *Bl*GrpE was calculated to be 91.7 ± 3.9 kcal/mol; however, this value was reduced to <52 kcal/mol in the inactive variants. Principally, the stability of the native state results from a balance between enthalpy and entropy. It has been demonstrated that the stabilization of proteins is mostly accompanied by a decrease in ΔS [44]. In our case, we should pay attention to the entropic increase of the unfolded state of the mutant *Bl*GrpEs relative to that of the wild-type protein (Table 2). An increase in the entropy of the inactive variants implies that the relevant substitutions have a detrimental effect on the thermostability of *Bl*GrpE. Proteins are only marginally stable since the free energy of stabilization ($\Delta G_{N\rightarrow U}$) ranges within 7.1–15.4 kcal/mol and is therefore equivalent to

Table 2 Thermodynamic parameters of wild-type and mutant *Bl*GrpEs

Enzyme	T_m (°C)[a]	ΔH_{nu} (kcal/mol)[b]	ΔS_{nu} (cal/mol/K)[c]	ΔG_{nu} (kcal/mol)[d]
Wild-type	58.0 ± 0.1	91.7 ± 3.9	277.2	3.9
L134H	37.3 ± 0.5	32.6 ± 2.6	105.1	1.5
L134K	38.8 ± 0.6	30.4 ± 2.8	97.6	1.6
L134R	45.3 ± 0.7	51.6 ± 7.7	162.1	2.0
L134D	39.4 ± 0.6	37.7 ± 3.4	120.8	1.9
L134E	39.7 ± 1.0	37.8 ± 4.9	121.0	2.1
L134F	53.4 ± 0.1	114.7 ± 6.0	351.3	3.9
L134W	47.7 ± 0.1	83.5 ± 3.4	260.4	3.3
L134Y	43.4 ± 0.1	67.0 ± 2.2	211.9	4.8
L134C	46.2 ± 0.1	90.0 ± 3.8	281.8	2.7
L134N	39.4 ± 0.8	30.1 ± 4.4	96.5	1.7
L134Q	41.8 ± 0.2	44.2 ± 2.2	140.3	1.9
L134S	41.6 ± 0.5	35.7 ± 2.7	113.3	1.6
L134T	39.9 ± 0.1	57.3 ± 1.8	183.2	3.1
L134A	45.4 ± 0.1	83.6 ± 3.5	262.6	3.3
L134G	47.1 ± 0.2	72.1 ± 4.3	225.3	2.5
L134I	52.1 ± 0.1	79.4 ± 2.9	244.3	2.9
L134M	53.0 ± 0.2	101.9 ± 4.4	312.7	3.6
L134P	35.6 ± 0.5	18.3 ± 3.9	59.2	0.4
L134V	48.8 ± 0.1	70.9 ± 2.5	220.2	3.5

[a] T_m, midpoint of the thermal unfolding transition

[b] ΔH_{nu}, difference in the van't Hoff enthalpy between the native and unfolded proteins

[c] ΔS_{nu}, difference in the entropy between the native and unfolded proteins

[d] ΔG_{nu}, difference in free energy between the native and unfolded proteins

only a few weak bonds [19]. Therefore, it is not surprising that their stability can be weakened through the lack of a few intramolecular interactions. As shown in Table 2, a significant reduction in $\Delta G_{N\rightarrow U}$ values of the inactive variants reflects that these mutant proteins are unstable in the native state.

4 Conclusion

In summary, the experimental data show how mutations of a single residue at the edge of α-helx 3 of *Bl*GrpE can affect its functionality. Interestingly, the alternative choices for position 134 of *Bl*GrpE could be phenylalanine, tryptophan, threonine, tyrosine, cysteine, isoleucine, methionine, and valine. The relevant replacements generate many variants with biochemical and biophysical characteristics comparable to wild-type *Bl*GrpE. Therefore, these results might provide a clue for the evolutionary trajectory of this protein group.

Acknowledgments This work was supported by National Science Council of Taiwan in Grant NSC 97-2628-B-415-001-MY3.

References

1. Adam H (1962) Adenosin 5'-diphosphat und Adenosin 5'-monophosphate. In: Bergmeyer HU (ed) Methoden der enzymatischen analyse. Verlag Chemie, Weinheim, pp 573–577
2. Alves VS, Pimenta DC, Sattlegger E, Castilho BA (2004) Biochem Biophys Res Commun 314:229–234
3. Armstrong Z, Reitinger S, Kantner T, Withers SG (2010) Chembiochem 11(4):533–538
4. Benaroudj N, Batelier G, Triniolles F, Ladjimi MM (1995) Biochemistry 34:15282–15290
5. Boshoff A, Stephens LL, Blatch GL (2008) Int J Biochem Cell Biol 40:804–812
6. Bradford MM (1976) Anal Biochem 72:248–254
7. Brehmer D, Rudiger S, Gassler CS, Klostermeier D, Packschies L, Reinstein J, Mayer MP, Bukau B (2001) Nat Struct Biol 8:427–432
8. Bukau B, Horwich AL (1998) Cell 92:351–366
9. Bukau B, Weissmam J, Horwich A (2006) Cell 125:443–451
10. Chen CC, Cho YC, Lai CC, Hsu WH (2009) J Agric Food Chem 57(15):6742–6747
11. Garcia-Ortega L, de Los Ríos V, Martinez-Ruiz A, Onaderra M, Lacadena J, Martinez del Pozo A, Gavilanes JG (2005) Electrophoresis 26:3407–3413
12. Gelinas AD, Langsetmo K, Toth J, Bethoney KA, Stafford WF, Harrison CJ (2002) J Mol Biol 323:131–142
13. Grimshaw JPA, Jelesarov I, Siegenthaler RK, Christen P (2001) J Biol Chem 276:6098–6104
14. Grimshaw JPA, Jelesarov I, Siegenthaler RK, Christen P (2003) J Biol Chem 278:19048–19053
15. Groemping Y, Klostermeier D, Herrmann C, Veit T, Seidel R, Reinstein J (2001) J Mol Biol 305:1173–1183
16. Eftink MR, Ramsay GD (1994) Methods Enzymol 240:615–645
17. Harrison CJ, Hoyer-Hartl M, Di Liberto M, Hartl F, Kuriyan J (1997) Science 276:431–435
18. Hartl FU, Hayer-Hartl M (2002) Science 295:1852–1858
19. Jaenicke R (1991) Eur J Biochem 202:715–728
20. Kotzia GA, Labrou NE (2009) FEBS J 276:1750–1761
21. Lanzett PA, Alvarez LJ, Reinach PS, Candia OA (1979) Anal Biochem 100:95–97
22. Liang WC, Lin MG, Chi MC, Chang HP, Lin LL (2009) Int J Biol Macromol 45:352–358
23. Liang WC, Lin MG, Chi MC, Hu HY, Lo HF, Chang HP, Lin LL (2009) Arch Microbiol 191:583–593
24. Liberek K, Marszalek J, Ang D, Georgopoulos C, Zylicz M (1991) Proc Natl Acad Sci USA 88:2874–2878
25. Lobley A, Whitmore L, Wallace BA (2002) Bioinformatics 18:211–212
26. Mally A, Witt SN (2001) Nat Struct Biol 8:254–257
27. Mayer MP, Rüdiger S, Bukau B (2000) Biol Chem 381:877–885
28. Mayer MP, Schröder H, Rüdiger S, Paal K, Laufen T, Bukau B (2000) Nat Struct Biol 7:586–593
29. Mao D, Wachter E, Wallace BA (1982) Biochemistry 21:4960–4968
30. Mehl AF, Heskett LD, Jain SS, Demeler B (2003) Protein Sci 12:1205–1215
31. Miyazaki K, Arnold FH (1999) J Mol Evol 49:716–720
32. Moro F, Muga A (2006) J Mol Biol 358:1367–1377
33. Moro F, Taneva SG, Velázquez-Campoy A, Muga A (2007) J Mol Biol 374:1054–1064
34. Moussa CE, Wersinger C, Rusnak M, Tomita Y, Sidhu A (2004) Neurosci Lett 371:239–243
35. Nakamura A, Takumi K, Miki K (2010) J Mol Biol 396:1000–1011
36. Packschies L, Theyssen H, Buchberger A, Bukau B, Goody RS, Reinstein J (1997) Biochemistry 36:3417–3422
37. Padhi SK, Bougioukou DJ, Stewart JD (2009) J Am Chem Soc 131(9):3271–3280
38. Popp SL, Reinstein J (2009) FEBS Lett 583:575–578
39. Schönfeld HJ, Schmidt D, Schröder H, Bukau B (1995) J Biol Chem 270:2183–2189
40. Siegenthaler RK, Christen P (2005) J Biol Chem 280:14395–14401
41. Sugimoto S, Higashi C, Yoshida H, Sonomoto K (2008) Protein Exp Purif 60:31–36
42. Sugimoto S, Saruwatari K, Higashi C, Sonomoto K (2008) Microbiology 154:1876–1885
43. Suh WC, Lu CZ, Gross CA (1999) J Biol Chem 274:30534–30539
44. Vieille C, Zeikus JG (2001) Trends Biotechnol 14:183–190
45. Whitmore L, Wallace BA (2004) Nucleic Acids Res 32:W668–W673
46. Willmund F, Mühlhaus T, Wojciechowska M, Schroda M (2007) J Biol Chem 282:11317–11328
47. Wu B, Wawrzynow A, Zylicz M, Georgopoulos C (1996) EMBO J 15:4806–4816
48. Zmijewski MA, Skórko-Glonek J, Tanfani F, Banecki B, Kotlarz A, Macario AJ, Lipińska B (2007) Acta Biochim Pol 54:245–252